Ciprofloxacin remediation by photolysis, TiO_2 photocatalysis and high-voltage electrical discharges: kinetics, energy demand and ecotoxicity

Cristèle DELSART

c.delsart@istom.fr

ISTOM - École supérieure d'agro-développement international

Maryline PFLIEGER

University of Nova Gorica

Urška LAVRENČIČ ŠTANGAR

University of Ljubljana

Nadia BOUSSETTA

Université de Technologie de Compiègne

Marwa BRAHIM

Univ. Bordeaux, CNRS, Bordeaux INP, EPOC, UMR 5805

Aurélien TRIVELLA

Univ. Bordeaux, CNRS, Bordeaux INP, EPOC, UMR 5805

Research Article

Keywords: Ciprofloxacin, degradation, photolysis, photocatalysis, electrical discharges, toxicity

Posted Date: July 8th, 2026

DOI: https://doi.org/10.21203/rs.3.rs-10081212/v1

Additional Declarations: No competing interests reported.

Abstract

This study investigated three advanced oxidation processes for Ciprofloxacin (CIP) water treatment: photolysis (PL), TiO_2 photocatalysis (PC), and high voltage electrical discharges (HVED). The research comprehensively evaluated degradation performances, electrical energy consumption, and ecotoxicological impacts. Comparative analysis revealed PC as the most effective treatment method. Half-life measurements of ciprofloxacin showed significant differences: PL (14.1 min), HVED (13.9 min) and PC (2.6 min). Notably, PC exhibited superior mineralization capabilities, achieving 25 times faster non-purgeable organic carbon (NPOC) reduction compared to photolysis and 2 times faster than HVED. Electrical energy consumption assessments further substantiated PC's efficiency. To attain 90% degradation of CIP, the process consumed less energy, with photolysis and HVED requiring 4.5 and 2.2 times more energy, respectively. Ecotoxicological evaluation involved three distinct organism types: *Vibrio fischeri* (bioluminescent bacteria), *Daphnia magna* (planktonic crustacean), and *Trifolium repens* (plant). Short-duration treatments (15–30 minutes) revealed increased toxicity. Luminescence inhibition in *Vibrio fischeri* and immobilisation of *Daphnia magna* suggested that intermediate degradation products were more toxic than the parent CIP molecule. Interestingly, a less pronounced toxic effect was observed on *Trifolium repens* compared to aquatic organisms, highlighting the complex ecological implications of water treatment processes. These findings provide crucial insights into advanced oxidation technologies for water remediation.

1. Introduction

Ciprofloxacin, a member of the second-generation quinolone family, has become one of the most widely used antibiotics worldwide in human and veterinary medicine, as well as in aquaculture (Brar et al. 2020; Gauba and Saxena 2023; Sharma et al. 2017; Yang et al. 2021). Its effectiveness is based on a broad spectrum of activity, covering both Gram-positive and Gram-negative bacteria, along with a targeted mechanism of action that inhibits bacterial DNA synthesis (Brar et al. 2020; Gauba and Saxena 2023). This specific action, ensuring strong antibacterial potency, has led to the intensive use of ciprofloxacin in the prevention and treatment of infectious diseases (Gauba and Saxena 2023). However, this pervasive presence, combined with massive and often uncontrolled use, results in the accumulation of large quantities of unmetabolized residues in the environment, causing harmful effects on ecosystems and human health (Cui et al. 2014; Gauba and Saxena 2023; Kim et al. 2020; Yang et al. 2021). Indeed, up to 70% of these antibiotics, including ciprofloxacin, can be excreted unchanged in urine and feces and subsequently reach wastewater, sludge, sediments, surface and groundwater, and in some cases even drinking water (Van Doorslaer et al. 2014; Yang et al. 2021).

The growing presence of ciprofloxacin in natural environments, often at trace levels ranging from nanograms to micrograms per liter, raises serious concerns, not only due to its potential impact on public health but also because of its ecological consequences (Yang et al. 2021). The very fact that this substance, initially developed to combat pathogenic bacteria, disperses into the environment and affects non-target microbial communities highlights new challenges related to aquatic pollution (Cui et al. 2014; Gauba and Saxena 2023; Kim et al. 2020). Due to its complex chemical structure, ciprofloxacin can disrupt ecosystem balance by altering soil microorganism distribution, modifying the bacteria/fungi ratio, and impacting the structure and functioning of microbial communities in wastewater treatment plants (Cui et al. 2014; Gauba and Saxena 2023; Kim et al. 2020). This disruption contributes to the development of antibiotic resistance, a major public health issue resulting from the continuous and inadequate exposure of microorganisms to these compounds (Gauba and Saxena 2023; Yang et al. 2021).

Moreover, ciprofloxacin is directly toxic to living organisms. It can induce increased production of aldehydes and peroxynitrites, provoke oxidative stress, and lead to cell death (Gauba and Saxena 2023; Leichtweis et al. 2022). The generated free radicals damage the mitochondrial DNA of mammalian cells and alter mitochondrial function (Gauba and Saxena 2023; Leichtweis et al. 2022). This cascade of effects spreads throughout the body’s organs, representing a latent health hazard. Its harmful effects are not limited to fauna and flora. The accumulation of ciprofloxacin residues in

the food chain, particularly in fish or in food crops irrigated with contaminated water, poses a risk to humans (Gauba and Saxena 2023). The residual presence of this antibiotic in food may encourage the emergence and spread of resistant bacteria, making antibiotic treatments less effective and undermining medical progress in combating infections (Gauba and Saxena 2023; Yang et al. 2021).

In response to these challenges, remediation and removal methods aimed at reducing environmental concentrations of ciprofloxacin, and more generally of fluoroquinolones, are under study. Conventional approaches such as coagulation, flocculation, sedimentation, filtration, chlorination, or ozonation may reduce ciprofloxacin levels in water, but their efficiency is often incomplete and highly dependent on operating conditions. In addition, some of these processes mainly transfer the pollutant to another phase rather than fully degrading it, while oxidative treatments may generate potentially toxic transformation by-products, and large-scale implementation can involve substantial infrastructure and operating costs (Gauba and Saxena 2023; Yang et al. 2021; Zambrano et al. 2022). Other solutions are emerging, emphasizing the sustainable and effective nature of bioremediation and phytoremediation (Gauba and Saxena 2023). The use of plants like vetiver or Indian mustard (Brassica juncea), as well as adapted microorganisms, has shown the capability to remove or degrade ciprofloxacin, offering a greener, more cost-effective, and more environmentally friendly alternative (Gauba and Saxena 2023). However, while bioremediation and phytoremediation are promising, they often proceed slowly and are heavily dependent on environmental conditions (Gauba and Saxena 2023; Yang et al. 2021). As a result, there is a strong interest in developing faster, more innovative, and more controllable methods to mitigate pollution.

Among the cutting-edge technologies recently explored, photolysis, photocatalysis, and high-voltage electrical discharges (HVED) stand out (Hong et al. 2022, 2023; Yang et al. 2021; Zambrano et al. 2022). These techniques are advanced oxidation processes, aiming to generate highly reactive hydroxyl radicals and other oxidizing species in situ, capable of attacking the chemical bonds of ciprofloxacin molecules. Thus, beyond mere removal by capture or separation, these methods enable genuine degradation, ideally approaching complete mineralization and preventing the formation of problematic residues (Yang et al. 2021; Zambrano et al. 2022).

Photolysis, a natural phenomenon enhanced by the input of light energy, can degrade certain organic compounds. Exposure to a light source, particularly ultraviolet (UV) light, promotes the breaking of chemical bonds and the transformation of pollutant molecules into simpler metabolites (Yang et al. 2021). In the case of ciprofloxacin, the presence of photosensitizers such as humic substances can accelerate the photodegradation rate (Porras et al. 2016). Studies have shown that these humic substances, naturally occurring in the environment, can improve system reactivity, reduce the pollutant's half-life, and thus stimulate its elimination (Porras et al. 2016). However, while photolysis can be effective, the photodegradation products may sometimes retain a degree of biotoxicity (Sturini et al. 2015, 2016). Therefore, it is essential to continue research to precisely identify the formed products and assess their impact on living organisms, ensuring that the proposed solution genuinely resolves the issue rather than merely transforming it (Yang et al. 2021).

Photocatalysis goes further by incorporating a catalyst, often a semiconductor such as titanium dioxide (TiO_2), to intensify the effect of light (Yang et al. 2021; Zambrano et al. 2022). Under light irradiation, electron-hole pairs are generated, promoting the formation of hydroxyl radicals and also other reactive oxygen species that attack the ciprofloxacin molecule. The advantage of photocatalysis lies in its capacity to mineralize a wide variety of recalcitrant organic compounds under relatively mild conditions (Zambrano et al. 2022). TiO_2, widely used for its abundance, stability, and non-toxicity, has been extensively studied for degrading various organic pollutants and could represent a promising technological approach for ciprofloxacin removal (Yang et al. 2021; Zambrano et al. 2022). Moreover, the possibility of reusing the catalyst without significant loss of efficiency is a notable economic asset, reducing operational costs and enhancing the competitiveness of photocatalysis compared to other technologies (Zambrano et al. 2022). Although photocatalysis remains at the applied research stage, the progress made is encouraging and opens new perspectives for wastewater treatment (Yang et al. 2021; Zambrano et al. 2022).

High-voltage electrical discharges (HVED) also represent an innovative technology belonging to advanced oxidation processes (Hong et al. 2022, 2023). Plasma plays a key role in these methods. Generating electrical discharges in or at the water surface produces a low-temperature plasma containing powerful oxidizing species — hydroxyl radicals and hydrogen peroxide — that can efficiently degrade ciprofloxacin molecules (Hong et al. 2022, 2023). The main advantage of this method lies in its ability to combine diverse physical and chemical effects without adding chemical agents, while limiting the production of undesirable by-products. Studies conducted on other contaminants, such as atrazine, have shown remarkable effectiveness, suggesting that this approach may also prove to be very promising for ciprofloxacin (Hong et al. 2022, 2023). However, HVED technology is still limited at the laboratory scale and requires further research, particularly to ensure the final safety of the resulting products.

Given the urgency of developing effective and sustainable degradation processes, it is essential to have approaches capable not only of reducing ciprofloxacin concentrations but also of ensuring optimal mineralization, thereby limiting the formation of persistent and/or toxic by-products (Gauba and Saxena 2023; Yang et al. 2021). Current knowledge indicates that while existing solutions are encouraging, they require comprehensive evaluation considering their efficiency, energy costs, ecological impact and their capacity to generate less harmful transformation products (Yang et al. 2021). A thorough analysis of the properties and degradation mechanisms, the substances formed during the process, and their potential toxicity is essential (Gauba and Saxena 2023; Sturini et al. 2015, 2016). Such a level of understanding, combined with targeted characterization methods, will ensure that we go beyond merely reducing pollution to genuinely improving the quality of aquatic environments over the long term (Yang et al. 2021).

Within this context, the present work proposes to compare three promising techniques for ciprofloxacin degradation: photolysis, photocatalysis, and high-voltage electrical discharge. These advanced oxidation methods offer distinct prospects in terms of mechanisms of action, overall efficiency, energy consumption, and the influence on the toxicity of their degradation products (Yang et al. 2021; Zambrano et al. 2022; Hong et al. 2022, 2023). This study aims to establish a comprehensive comparative assessment that determines the quantitative removal of ciprofloxacin, the mineralization level and the evaluation of residual ecotoxicity.

2. Materials and methods

2.1 Chemicals

Ciprofloxacin (CIP, CAS No 86483-48-9, > 98%) was purchased from Fluorochem. The water used for the preparation of the solutions is produced by a Milli-Q water purification system (PURELAB Flex, UK) producing purified water with a pH of 6.2, resistivity of 18.2 MΩ.cm and TOC < 5 ppb.). Salts used for the preparation of synthetic freshwater were calcium chloride dihydrate (p.a., Kemika), magnesium sulfate heptahydrate (> 99,5%, Fisher Chemical), sodium bicarbonate (> 99,5%, Kemika), and potassium chloride (> 99,0%, Gram-Mol)).

2.2 Degradation experiments

To simulate a simplified natural freshwater medium, ciprofloxacin solutions at 50 mg/L were prepared in synthetic freshwater (pH = 7.2) according to the protocol described in OECD guideline No. 202 (OECD 2004). This protocol involves the preparation of four stock solutions containing 11.76 g of $CaCl_2 \cdot 2H_2O$, 4.93 g of $MgSO_4 \cdot 7H_2O$, 2.59 g of $NaHCO_3$, and 0.23 g of KCl, respectively, in one liter of deionized water. Subsequently, 25 mL of each solution were withdrawn and added to 1 L of deionized water.

Under “dark conditions”, i.e., without light or electric discharges, all treatments exhibited negligible CIP loss (< 4%), confirming that the observed concentration decreases result from molecular degradation during the active experiments (Online Resource 1).

For each process, the electrical energy consumed to treat one cubic meter of water (Ec, kWh/m³) was determined using the following equation:

$E_c = (P \times t) / V$ (1)

where P is the applied power, t is the treatment time (h), and V is the volume of the treated sample (m^3).

2.2.1 Photolysis experiments

Photolysis experiments were carried out in a circular photoreactor as described by Černigoj et al. (Černigoj et al. 2007). In brief, the reactor consisted of a double-walled glass tube (240 mm in length, 40 mm inner diameter) placed in the center of a circular stainless-steel enclosure equipped with six low-pressure mercury fluorescent lamps acting as a UV-A radiation source (CLEO 20 W, 438 mm x 26 mm, Philips; broad emission maximum at 355 nm). The photoreactor, which had an effective volume of 250 mL, was connected to a circulating water bath (Haake SC100/A25, Thermo Scientific) to maintain a constant temperature of 25 ± 0.5°C throughout the experiments. Samples were oxygenated with synthetic air (5.0, Messer) and irradiated for fixed periods of time as follows: 0, 10, 20, 30, 45, 60, and 90 min.

2.2.2 Photocatalysis experiments

Photocatalytic experiments were conducted in the same photoreactor as described above (section 2.2.1). However, an additional holder made entirely of Teflon was inserted into the tube. Eight glass slides with immobilised TiO_2 photocatalyst were fastened around the axis of the holder. Transparent anatase-TiO_2 films (a mixture of TiO_2 P25 (Aeroxide, Evonik Industries) and PC500 (Cristal Global, Millennium Inorganic Chemicals) (50/50, w/w)) were deposited on both sides of soda-lime glass slides (175 mm × 12.5 mm × 2 mm, total surface area of 43.75 cm²) and produced by a dip-coating process as previously described by Černigoj et al. (Černigoj et al. 2007). The average surface density of the coated TiO_2 was 1.2 ± 0.4 mg/cm², which corresponds to 420 mg of immobilised photocatalyst in total for each experiment. First, the coated slides were immersed in the sample solution for 40 min in the dark to allow CIP to equilibrate between the aqueous and solid phases. Subsequently, samples were irradiated for fixed periods of time as follows: 0, 2.5, 5, 7.5, 10, 12.5, 15, 17.5, 20, 25, 30, 45, and 60 min at 25 ± 0.5°C.

2.2.3 High voltage electrical discharges experiments (HVED)

The HVED equipment consists of a cylindrical Teflon treatment chamber (1 L, inner diameter of 110 mm) equipped with rod-to-plane geometry electrodes connected to a high-voltage pulse generator (Basis, St Quentin, France). The electrodes were made of stainless steel. The diameters of the upper and lower electrodes were 10 mm and 30 mm, respectively, with an inter-electrode distance of 5 mm. The high-voltage generator (40 kV, 10 kA) provided damped oscillation pulses.

The effective electric field strength was defined as $E_{effective} = U/d_{inter-electrodes}$. The effective HVED treatment time ($t_{HVED\ effective}$, µs) was calculated as the product of the average pulse width (t_i, µs) and the number of pulses (n). The nominal HVED treatment time (t_{HVED}, min) corresponded to the total treatment duration. The pulse width (t_i) was approximately 10 µs. The specific energy input (W, J/L) was determined using the following equation:

$W = (n \times P_i) / V$ (2)

where V is the volume of the treated sample (L) and P_i is the energy of a single electric pulse (240 J).

Different treatment times (t_{HVED}) were tested during this study and the details of these experimental conditions are presented in Table 1. The solution (250 mL) was introduced into the chamber immediately prior to the HVED treatment. Before and after treatment, the temperature ($T_{initial/final}$, °C) of the samples in the treatment chamber was measured using a Teflon-coated K-type thermocouple (± 0.1°C) connected to a data logger thermometer (Center 305/306, JDC Electronic

SA, Switzerland). To prevent excessive heating during the HVED treatment, a 5 min pause was implemented every 25 min. Subsequently, the samples were filtered through a glass filter funnel (100 mL, porosity 16–40 µm, Duran), placed in containers, and stored at 4°C until analysis.

Table 1
Modalities of HVED treatments (n: number of pulses; t_{HVED}: HVED treatment time; $t_{HVED\ effective}$: effective HVED treatment time; W: energy input; ΔT: temperature difference before and after treatment)

n	**0**	**167.2**	**172.4**	**204.9**	**216.7**	**234.5**	**312.5**	**403.2**	**466.7**	**560.5**	**641.0**	**800**
t_{HVED}, *min*	0	13.9	14.4	17.1	18.1	19.5	26.0	33.6	38.9	46.7	53.4	66.7
$t_{HVED\ effective}$, ms	0	1.7	1.7	2.0	2.2	2.3	3.1	4.0	4.7	5.6	6.4	8.0
W, kJ/L	0	161	166	197	208	225	300	387	448	538	615	768
ΔT, °C	0.5	5	6	6	7	6	15	17	8	5	23	26

2.3 Ecotoxicity assays

The ecotoxicity of the samples was assessed on 3 organisms belonging to different trophic levels: *Trifolium repens*, *Daphnia magna*, *Vibrio fischeri* (Table 2). Each set of tests was performed against a control composed of synthetic freshwater. Sample aliquots were taken at the beginning and at the end of each test to ensure that CIP concentration was maintained within 10% of the measured initial concentration throughout the assay. Measurements were tested using one-way analysis of variance (one-way ANOVA) followed by the Scheffé post hoc test in order to identify significant differences between the initial solution (CIP at time 0) and the degradation mixtures (Qi Macros 2017).

Table 2
Characteristics of the ecotoxicity tests

Organisms	**Test type**	**Test duration**	**Test criterion**
Trifolium repens	Acute	6 days	Root length and sprouted seeds
Vibrio fischeri	Acute	15 and 30 min	Luminescence inhibition
Daphnia magna	Acute	48 h	Immobilisation

2.3.1 Test organism *Trifolium repens*

Germination inhibition and root growth tests were carried out on seeds of *Trifolium repens* (white clover – Semenarna Ljubljana, Slovenia) according to a protocol adapted from Lin and Xing (Lin and Xing 2007). Briefly, seeds were soaked in DI-water prior to use. Filter paper was placed into Petri dishes (100 mm x 15 mm) and 2.5 mL of sample was added. Ten seeds were transferred on the paper and arranged at least 1 cm away from each other to ensure enough space for each seed to germinate. Petri dishes were then covered, sealed and placed in the dark at 21 ± 1°C. After 6 days, when at least 80% of the control seeds had sprouted, the number of germinated seeds was counted and the root length measured. Each sample was tested in 4 replicates. Median values with first and third quartiles as uncertainty were considered for data processing.

2.3.2 Test organism *Daphnia magna*

Acute immobilisation test was performed on *Daphnia magna* (a single laboratory colony cultured at 21 ± 1°C) according to OECD guideline n°202 (OECD 2004). Test vessels were filled with 20 mL of samples and 5 individual daphnids (less than 24 h old) were introduced in each of the vessels. All vessels were placed in the dark at 21 ± 1°C. After 48 h of incubation (without feeding), the number of mobile daphnids (i.e. perceptible movement in 15 s of observation per animal) was counted in each vessel. For a set of tests to be valid, at least 90% of the daphnids should still be mobile in the control vessels. Average values with standard deviation of four replicates per sample were considered for data processing.

2.3.3 Test organism *Vibrio fischeri*

The inhibitory effect of the samples on the bioluminescence of the marine bacterium *Vibrio fischeri* (NRRL B–11177, Hach Dr. Lange GmbH, Germany) was determined following the international standard ISO 11348-2:2007 (ISO 11348-2:2007). As a pre-treatment, the pH and salinity of the samples were adjusted to 7 ± 0.2 and 2% (w/v) sodium chloride (NaCl, ACS reagent, ≥ 99.8%), respectively. For each test, 7 mixtures of bacteria with samples were prepared by cascade dilution. The light emission inhibition was determined against a non-toxic control (2% NaCl with adjusted pH) after 15 and 30 min incubation times. For a positive control, potassium dichromate (K2Cr2O7, ACS reagent, ≥ 99.0%) was used as specified in the ISO standard protocol. The light emitted by the bacteria in the mixtures and controls was measured with a photomultiplier (LUMIStox 300 luminometer, Hach Dr. Lange GmbH, Germany) equipped with a thermoblock set at (15 ± 1) °C (LUMIStherm, Hach Dr. Lange GmbH, Germany). Tests which did not comply with all the validity criteria (ISO 11348-2:2007) (ISO 11348-2:2007) were discarded. The obtained data were treated by LUMISsoft 4 software applying a colour correction. Each sample was tested in 3 double-determination replicates. Average values with standard deviation of the replicates were considered for data processing.

2.4 Analytical methods

CIP concentrations were determined by High-Performance Liquid Chromatography (HPLC, Agilent 1100 Series) equipped with a diode array detector (DAD) and a fluorescence detector (FLD). A 20-µL aliquot of the sample was injected into a Luna C_{18} column (150 × 4.6 mm, 3 µm) and its corresponding pre-column maintained at 26°C. The eluent flow rate was set at 0.8 mL/min. The mobile phase, composed of 0.1% formic acid (eluent A, Fluka, ≥ 98%) and acetonitrile (eluent B, Sigma-Aldrich, HPLC grade, ≥ 99.9%), was used in isocratic mode (88% A / 12% B, v/v). CIP was detected at 280 nm using the DAD. Fluorescence detection was performed at l_{ex} = 280 nm and l_{em} = 450 nm.

Non-purgeable organic carbon content was determined for each sample using a TOC analyzer (multi N/C 3100, Analytik Jena). Prior to analysis, the samples were acidified with hydrochloric acid (2 N, pH < 2) and purged with CO_2-free oxygen (5.0, Messer) to remove inorganic carbon and highly volatile organic compounds from the samples.

Anionic products (*i.e.*, nitrate and fluoride ions) formed during the degradation processes were quantified using ion chromatography (LC-10Ai, Shimadzu) with conductivity detection (CDD-10A, Shimadzu). The mobile phase was composed of HCO_3^- and CO_3^{2-}.

3. Results and discussion

3.1 Degradation of CIP by photolysis, TiO_2 photocatalysis, and HVED treatments

Figure 1a illustrates the kinetics of CIP degradation by photolysis (PL), TiO_2 photocatalysis (PC), and high voltage electrical discharge (HVED) treatments in synthetic freshwater. CIP degradation follows apparent first-order kinetics across all three processes. The data indicate that PL and HVED processes exhibit comparable efficiencies in degrading CIP, whereas PC is the most effective at degrading the antibiotic.

Apparent first-order rate constants, half-lives, and coefficients of determination are summarized in Table 3. The degradation of CIP shows satisfactory linearity, with coefficients of determination ranging from 0.980 to 0.992. The calculated half-lives are 14.1 minutes for PL, 13.9 minutes for HVED, and 2.6 minutes for PC. The fivefold decrease in half-life observed with the PC treatment compared to the other two processes is consistent with the high reactivity of the antibiotic to oxidation reactions (Pretali et al. 2022). Specifically, PC induces the formation of hydroxyl radicals that subsequently degrade CIP.

Table 3
Apparent first-order rate constants (k_{app}, min^{-1}), half-lives (t1/2, min), and coefficients of determination calculated from degradation and non-purgeable organic carbon (NPOC) kinetics during CIP photolysis (PL), TiO_2 photocatalysis (PC), and HVED treatments in synthetic freshwater.

Treatment	**Degradation**			**NPOC**		
	k_{app} (min^{-1})	**$t_{½}$ (min)**	**R^2**	**k_{app} (min^{-1})**	**$t_{½}$ (min)**	**R^2**
PL	0.049	14.1	0.984	$7x10^{-4}$	990.2	0.916
PC	0.267	2.6	0.992	$17.7x10^{-3}$	39.2	0.949
HVED	0.050	13.9	0.980	$8.5x10^{-3}$	81.5	0.892

To better compare the three treatments, the concentration of fluoride ions was monitored as a function of CIP reaction time (Fig. 1b). Nucleophilic substitution of fluorine is one of the main chemical pathways for the degradation of fluoroquinolones (Pretali et al. 2022; Tyutereva et al. 2024). Monitoring the concentration of fluoride ions allows for an assessment of the extent to which this mechanism contributes to CIP degradation depending on the process used. Figure 1b clearly demonstrates that this reaction pathway is highly favoured in both photochemical processes, i.e., PL and PC, with fluoride ion concentrations approaching 3.5 mg/L after 60 minutes of reaction. In contrast, the HVED process yields a concentration of approximately 2.0 mg/L over the same period. Therefore, the contribution of nucleophilic substitution to CIP degradation is less significant during the HVED process.

Monitoring the concentrations of non-purgeable organic carbon and nitrate ions provides complementary information for understanding CIP degradation (Fig. 2), particularly its mineralization. The apparent first-order kinetics for non-purgeable organic carbon removal are presented in Fig. 2a. We observed an increase in mineralization efficiency in the order of PL to HVED to PC. Furthermore, the apparent first-order rate constants, half-lives, and coefficients of determination calculated from the non-purgeable organic carbon kinetics are summarized in Table 3. As expected, the kinetics exhibited poor linearity, with R^2 values ranging from 0.892 to 0.949. However, the reliability of the data is sufficient to compare the three treatments. The results show that PL is inefficient in CIP mineralization; specifically, the time required to mineralize 50% of the initial CIP amount is 990.2 minutes. The HVED process achieves CIP mineralization 12 times faster than PL ($t_{1/2}$ = 81.5 min). This result, combined with the data presented in Fig. 1a showing that both processes have comparable half-lives for CIP degradation, indicates that PL induces less mineralization than HVED. Finally, PC ($t_{1/2}$ = 39.2 min) mineralizes CIP 25 and 2 times faster than PL and HVED, respectively. Therefore, PC is the most efficient process in terms of both CIP degradation kinetics and mineralization.

The evolution of nitrate ion concentration exhibits varying behaviors depending on the treatment applied (Fig. 2b). Over the course of the reaction, PL treatment yielded no detectable nitrate ions, clearly demonstrating that PL does not significantly mineralize CIP within the experimental duration, as previously indicated by non-purgeable organic carbon results. In contrast, both PC and HVED treatments induce the formation of nitrate ions from CIP degradation, although their concentration trends differ markedly. In the case of HVED, nitrate ions are observed after 18 minutes of reaction. Subsequently, a first plateau is reached with a concentration of approximately 1.3 mg/L after 39 minutes. Finally, a

second stage is attained after 47 minutes, with the concentration increasing to 2.9 mg/L. For PC, nitrate ions are detected only after 30 minutes. Thereafter, the concentration rapidly increases, reaching 3.8 mg/L after 60 minutes of reaction. Both processes effectively mineralize the antibiotic under study. While HVED appears to act faster initially in terms of CIP mineralization, PC surpasses it at reaction times exceeding 47 minutes and ultimately achieves a higher level of mineralization at extended reaction times.

These results, supported by apparent first-order kinetics, clearly demonstrate that CIP degradation proceeds more rapidly with PC compared to PL and HVED. Moreover, the mineralization of CIP reaches a higher level with PC, as indicated by the corroborating results from non-purgeable organic carbon measurements and nitrate ions concentration analyses. Finally, the nucleophilic substitution reaction of fluorine was observed in all three treatments and does not constitute a selective mechanism for advancing CIP mineralization.

It should be noted that all experiments were conducted in synthetic freshwater, which provides standardized and reproducible conditions but does not fully reflect the chemical complexity of natural waters. Dissolved organic matter, commonly present in environmental aqueous matrices, can hinder the effectiveness of these processes, reducing their pollutant degradation efficiency (Matoh et al. 2023). Consequently, the CIP degradation and mineralization efficiencies reported herein likely represent an upper-bound scenario, whereas decreased performance would be expected in natural waters.

3.1.1 Comparison of the electrical energy consumption

One of the primary criteria for selecting a suitable remediation process is the associated electrical energy consumption, which has been thoroughly evaluated herein. Figure 3 illustrates the variation in electrical energy consumption for each treatment as a function of CIP degradation. Regardless of the percentage of degradation achieved, the energy consumption hierarchy remains consistent: PC consumes the least energy, HVED exhibits an intermediate consumption level, and PL is the most energy-intensive process. To achieve 90% degradation of CIP, the energy required is approximately 300, 149 and 67 kWh/m³ for the PL, HVED and PC processes, respectively. Specifically, PL consumes 4.5 times more energy than PC, while HVED consumes 2.2 times more. Therefore, from an energy efficiency standpoint, PC emerges as the most favorable among the evaluated processes.

Although the energy demand associated with PC is the lowest among the processes tested, it remains substantial, potentially even prohibitive for widespread large-scale application. In contrast, ozonation, a conventional remediation process, has an energy requirement ranging from only 0.03 to 0.15 kWh/m³ (Grzegorzek et al. 2023), making it highly economical in terms of energy consumption. However, when factoring in the environmental and human health costs arising from the presence of organic micropollutants in natural waters, along with the superior remediation efficiency of PC compared to traditional processes, the balance may tilt in favor of PC. Despite its higher energy requirements, PC ultimately offers greater long-term environmental benefits.

3.2 Ecotoxicity experiments

3.2.1 Evolution of ecotoxicity on *Vibrio fischeri*

The tests conducted on *Vibrio fischeri* (Fig. 4a, b) reveal a contrasting evolution in bioluminescence inhibition during the degradation of ciprofloxacin (CIP).

At the initial photolysis times (t = 0, 10, 20 min), negative inhibition values are observed, suggesting a slight stimulation of bacterial bioluminescence. This indicates that, during these early times, the bacterial mortality rate is lower than the growth rate. However, when photolysis continues (t ≥ 60 min), the inhibition becomes positive and significant (up to 16–

20%), indicating the likely formation of photodegradation by-products capable of stressing the bacteria (Sturini et al. 2015, 2016).

During the initial minutes of photocatalytic treatment (t = 0, 2.5 min), inhibition is low (or even negative), then increases as treatment time progresses (up to 15–18% at t ≥ 10 min). This increase in inhibition reflects the formation of potentially toxic degradation intermediates (Yang et al. 2021; Zambrano et al. 2022).

Samples treated with high-voltage electrical discharges show a steady increase in bioluminescence inhibition over time (up to 20–30% at t > 30 min). Hydroxyl radicals generated by the plasma (Hong et al. 2022, 2023) degrade CIP, but the formation of certain by-products (e.g., hydroxylated aromatic compounds) may explain the observed increase in inhibition before these intermediates are further transformed (Yang et al. 2021).

Thus, for *Vibrio fischeri*, all three processes show a generally increasing effect on luminescence inhibition as CIP degradation progresses. This initial rise in toxicity is frequently reported in the literature for antibiotics from the fluoroquinolone family (Sturini et al. 2015, 2016). However, it is important to note that the bioluminescence tests at 15 (Online Resource 2) and 30 min provide only a snapshot of toxicity: prolonged treatment can ultimately reduce overall toxicity due to more complete mineralization (Zambrano et al. 2022).

3.2.2 Evolution of toxicity in *Daphnia magna*

The immobilisation test on *Daphnia magna* (OECD 2004) was used to assess the fraction of immobile daphnids after 48 hours of exposure to water samples treated with the three degradation processes (Fig. 5a, b).

While the initial CIP solution (t = 0) causes approximately 5% immobilisation (in line with literature values indicating moderate toxicity at these concentrations, (Gauba and Saxena 2023)), increasing photolysis time leads to a rise in immobilisation (up to 75% at t = 90 min). This confirms that photolysis by-products, which are poorly mineralized, can be more toxic to aquatic organisms (Sturini et al. 2015, 2016).

With photocatalysis, trends are more variable. At 5 minutes, high mobility is observed (90%), while at other times (e.g., 12.5 min), immobilisation reaches 65%. This fluctuation likely reflects the coexistence of degradation intermediates with contrasting toxicities (Zambrano et al. 2022). Nevertheless, studies indicate that in the long term, photocatalysis tends to lead to the formation of less hazardous, more mineralized by-products (Yang et al. 2021).

Immobilisation also increases with treatment time under high-voltage electrical discharges (HVED), indicating the transient formation of compounds potentially more harmful than the parent CIP. Some values (around t ≈ 18 min) suggest up to 90% immobile daphnids. Subsequently, a slight decrease in immobilisation is sometimes noted, consistent with the gradual breakdown of the most toxic intermediates as treatment time progresses (Hong et al. 2022, 2023).

Overall, the sensitivity of *Daphnia magna* to degradation intermediates supports the findings obtained with *Vibrio fischeri*. Despite the eventual decrease in CIP, short-term treatments with incomplete mineralization can generate transient by-products that are more toxic than the initial compound (Yang et al. 2021).

3.2.3 Evolution of toxicity on *Trifolium repens*

The effects on seed germination and root growth of *Trifolium repens* (Lin and Xing 2007) were examined after 6 days of exposure to the treated samples (Fig. 6a-d).

The roots of seedlings exposed to the initial CIP solution (*t* = 0) and to CIP degraded by photolysis (*t* = 90 min) showed relatively similar lengths (around 30 to 35 mm); root growth inhibition compared to the untreated control remained below

11%. The germination rate was affected (inhibition < 25%) at the times considered. However, it should be noted that these percentages sometimes conceal significant variability.

Toxicity toward *T. repens* varied after photocatalysis. The roots exhibited slight stimulation in growth (more than 26% increase in length compared to the untreated sample). In contrast, germination inhibition (ranging from 10 to 25%) was observed. However, these germination rates remained higher than the control. It is possible that some intermediate metabolites had either a beneficial effect (e.g., providing nutrients) or a harmful one (e.g., due to toxic compounds), depending on the specific experimental conditions (Zambrano et al. 2022).

The results obtained with HVED (High Voltage Electrical Discharges) showed more pronounced effects, with significantly reduced germination and root lengths at longer treatment times (up to 45% inhibition of germination and up to 31% inhibition of root growth). The observed variations highlight the importance of precisely characterizing the nature of the by-products formed (Hong et al. 2023).

Across all tests conducted with *T. repens*, the effects observed were much lower than those seen in aquatic microfauna, which is consistent with the generally lower sensitivity of many non-target plants compared to aquatic organisms (Gauba and Saxena 2023).

4. Conclusion

This research work assessed three treatment approaches: photolysis, TiO_2 photocatalysis, and High Voltage Electrical Discharge (HVED), focusing on kinetic performance and mineralization of organic micropollutant. This comparative study has clearly highlighted the superiority of the photocatalytic treatment for the degradation of CIP in synthetic freshwater. Indeed, regarding the degradation of this compound, the TiO_2 photocatalytic process is five times faster compared to the other two treatments, achieving 50% degradation of CIP in 2.6 minutes. Mechanistic analysis through fluoride ion formation confirmed that nucleophilic substitution predominantly occurs in photon-involved treatments. Furthermore, tracking the mineralization of CIP using non-purgeable organic carbon on the one hand and the formation of nitrate ions on the other clearly demonstrated that the TiO_2 photocatalytic treatment achieves the highest level of mineralization among the tested processes. Indeed, the time required to mineralize 50% of the initial quantity of CIP by the TiO_2 photocatalytic process is 25 times faster than photolysis and twice as rapidly as HVED. Monitoring the concentration of nitrate ions corroborated the previous results, although there is a nuance in the comparison between TiO_2 photocatalysis and HVED. In fact, the concentration of nitrate ions favors photocatalysis only after a certain reaction time. Finally, the energy evaluation of each process revealed that TiO_2 photocatalysis is 4.5 and 2.2 times less energy consuming than photolysis and HVED, respectively.

The toxicity tests conducted on *Vibrio fischeri* showed an increased toxicity in the case of HVED compared to photochemical processes. The latter favor nucleophilic substitution, whereas HVED also involves other mechanisms that could lead to more toxic molecular structures and/or higher concentrations. The results obtained from *Daphnia magna* also supported these observations, showing more significant immobilisation with HVED. Finally, the effects on seed germination and root growth of *Trifolium repens* are more nuanced. None of the three treatments clearly stand out.

To further deepen the understanding of the environmental impact of the presence of CIP in waters, it would also be interesting to identify the structures of the degradation products and study their toxicities individually.

Ultimately, the study provides comprehensive evidence of TiO_2 photocatalysis's potential in addressing micropollutant remediation, but further studies on combinations of processes could be implemented to try to improve the degradation rate and mineralization of CIP.

This research contributes significant insights into advanced water treatment technologies, highlighting the critical role of innovative photocatalytic approaches in mitigating organic micropollutant challenges.

Declarations

Competing interests

The authors have no relevant financial or non-financial interests to disclose.

Ethics approval

Not applicable.

Funding

The authors declare that no funds, grants, or other support were received during the preparation of this manuscript.

Author Contribution

C.D.: Conceptualization, Data curation, Formal analysis, Investigation, Methodology, Project administration, Visualization, Writing - original draft.M.P.: Conceptualization, Data curation, Investigation, Methodology, Writing - review and editing.U.L.S.: Resources, Supervision, Writing - review and editing.N.B.: Resources, Supervision, Writing - review and editing.M.B.: Validation, Writing - review and editing.A.T.: Formal analysis, Visualization, Writing - original draft.

Acknowledgement

The authors would like to thank Suzanna Žižek for her valuable assistance with the ecotoxicological analyses and Michael Shannon for proofreading and improving the English language of the manuscript.

Data availability

The data supporting the findings of this study are available within the article and its supplementary information files; additional data are available from the corresponding author upon reasonable request.

References

1. Brar RK, Jyoti U, Patil RK, Patil HC (2020) Fluoroquinolone antibiotics: an overview. Adesh Univ J Med Sci Res 2:26–30. https://doi.org/10.25259/AUJMSR_12_2020
2. Černigoj U, Lavrenčič Štangar U, Trebše P (2007) Evaluation of a novel Carberry type photoreactor for the degradation of organic pollutants in water. J Photochem Photobiol Chem 188:169–176. https://doi.org/10.1016/j.jphotochem.2006.12.009
3. Cui H, Wang S-P, Fu J, Zhou Z-Q, Zhang N, Guo L (2014) Influence of ciprofloxacin on microbial community structure and function in soils. Biol Fertil Soils 50:939–947. https://doi.org/10.1007/s00374-014-0914-y

4. Gauba P, Saxena A (2023) Ciprofloxacin properties, impacts, and remediation. CABI Rev 2023:1–8. https://doi.org/10.1079/cabireviews.2023.0005
5. Grzegorzek M, Wartalska K, Kaźmierczak B (2023) Review of water treatment methods with a focus on energy consumption. Int Commun Heat Mass Transf 143:106674. https://doi.org/10.1016/j.icheatmasstransfer.2023.106674
6. Hong J, Boussetta N, Enderlin G, Merlier F, Grimi N (2022) Degradation of residual herbicide atrazine in agri-food and washing water. Foods 11:2416. https://doi.org/10.3390/foods11162416
7. Hong J, Boussetta N, Enderlin G, Merlier F, Grimi N (2023) Degradation of herbicide atrazine in water by high voltage electrical discharge in comparison with Fenton oxidation and ultrasound treatments. RSC Sustain 1:1462–1470. https://doi.org/10.1039/D3SU00103B
8. ISO 11348-2:2007 (2007) Water quality - Determination of the inhibitory effect of water samples on the light emission of *Vibrio fischeri* (Luminescent bacteria test) - Part 2: Method using liquid-dried bacteria. International Organization for Standardization, Geneva
9. Kim D, Nguyen LN, Oh S (2020) Ecological impact of the antibiotic ciprofloxacin on microbial community of aerobic activated sludge. Environ Geochem Health 42:1531–1541. https://doi.org/10.1007/s10653-019-00392-6
10. Leichtweis J, Vieira Y, Welter N, Silvestri S, Dotto GL, Carissimi E (2022) A review of the occurrence, disposal, determination, toxicity and remediation technologies of the tetracycline antibiotic. Process Saf Environ Prot 160:25–40. https://doi.org/10.1016/j.psep.2022.01.085
11. Lin D, Xing B (2007) Phytotoxicity of nanoparticles: inhibition of seed germination and root growth. Environ Pollut 150:243–250. https://doi.org/10.1016/j.envpol.2007.01.016
12. Matoh L, Žener B, Kovačić M, Kušić H, Arčon I, Levstek M, Lavrenčič Štangar U (2023) Photocatalytic sol-gel/P25 TiO_2 coatings for water treatment: degradation of 7 selected pharmaceuticals. Ceram Int 49:24395–24406. https://doi.org/10.1016/j.ceramint.2022.09.204
13. OECD (2004) Test No. 202: Daphnia sp. acute immobilisation test. OECD Guidelines for the Testing of Chemicals, Section 2. OECD Publishing, Paris. https://doi.org/10.1787/9789264069947-en
14. Porras J, Bedoya C, Silva-Agredo J, Santamaría A, Fernández JJ, Torres-Palma RA (2016) Role of humic substances in the degradation pathways and residual antibacterial activity during the photodecomposition of the antibiotic ciprofloxacin in water. Water Res 94:1–9. https://doi.org/10.1016/j.watres.2016.02.024
15. Pretali L, Fasani E, Sturini M (2022) Current advances on the photocatalytic degradation of fluoroquinolones: photoreaction mechanism and environmental application. Photochem Photobiol Sci 21:899–912. https://doi.org/10.1007/s43630-022-00217-z
16. Sharma D, Patel RP, Zaidi STR, Sarker MMR, Lean QY, Ming LC (2017) Interplay of the quality of ciprofloxacin and antibiotic resistance in developing countries. Front Pharmacol 8:546. https://doi.org/10.3389/fphar.2017.00546
17. Sturini M, Speltini A, Maraschi F, Pretali L, Ferri EN, Profumo A (2015) Sunlight-induced degradation of fluoroquinolones in wastewater effluent: photoproducts identification and toxicity. Chemosphere 134:313–318. https://doi.org/10.1016/j.chemosphere.2015.04.081
18. Sturini M, Speltini A, Maraschi F, Profumo A, Tarantino S, Gualtieri AF, Zema M (2016) Removal of fluoroquinolone contaminants from environmental waters on sepiolite and its photo-induced regeneration. Chemosphere 150:686–693. https://doi.org/10.1016/j.chemosphere.2015.12.127
19. Tyutereva YE, Snytnikova OA, Sheven DG, Fedunov RG, Yanshole VV, Grivin VP, Pozdnyakov IP (2024) Mechanism of UV photodegradation of fluoroquinolone antibiotic ciprofloxacin in aqueous solutions. Chemosphere 367:143643. https://doi.org/10.1016/j.chemosphere.2024.143643
20. Van Doorslaer X, Dewulf J, Van Langenhove H, Demeestere K (2014) Fluoroquinolone antibiotics: an emerging class of environmental micropollutants. Sci Total Environ 500–501:250–269.

https://doi.org/10.1016/j.scitotenv.2014.08.075
21. Yang Q, Gao Y, Ke J, Show PL, Ge Y, Liu Y, Guo R, Chen J (2021) Antibiotics: an overview on the environmental occurrence, toxicity, degradation, and removal methods. Bioengineered 12:7376–7416. https://doi.org/10.1080/21655979.2021.1974657
22. Zambrano J, García-Encina PA, Jiménez JJ, López-Serna R, Irusta-Mata R (2022) Photolytic and photocatalytic removal of a mixture of four veterinary antibiotics. J Water Process Eng 48:102841. https://doi.org/10.1016/j.jwpe.2022.102841

Figures

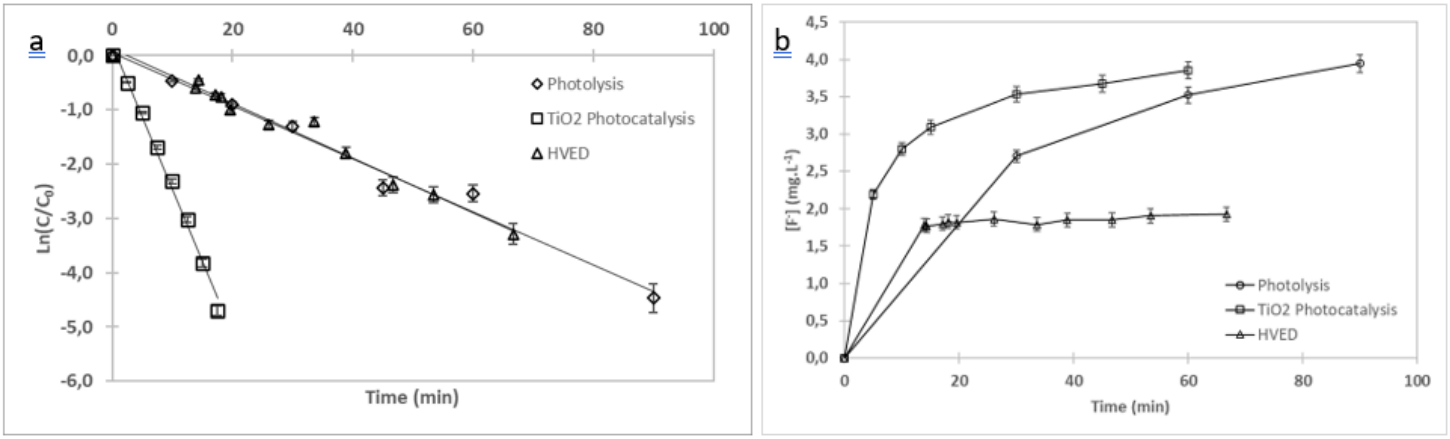

Figure 1

(a) Apparent first-order kinetics for CIP degradation and (b) concentrations of fluoride ions as a function of reaction time obtained from photolysis, TiO_2 photocatalysis, and HVED treatments in synthetic freshwater.

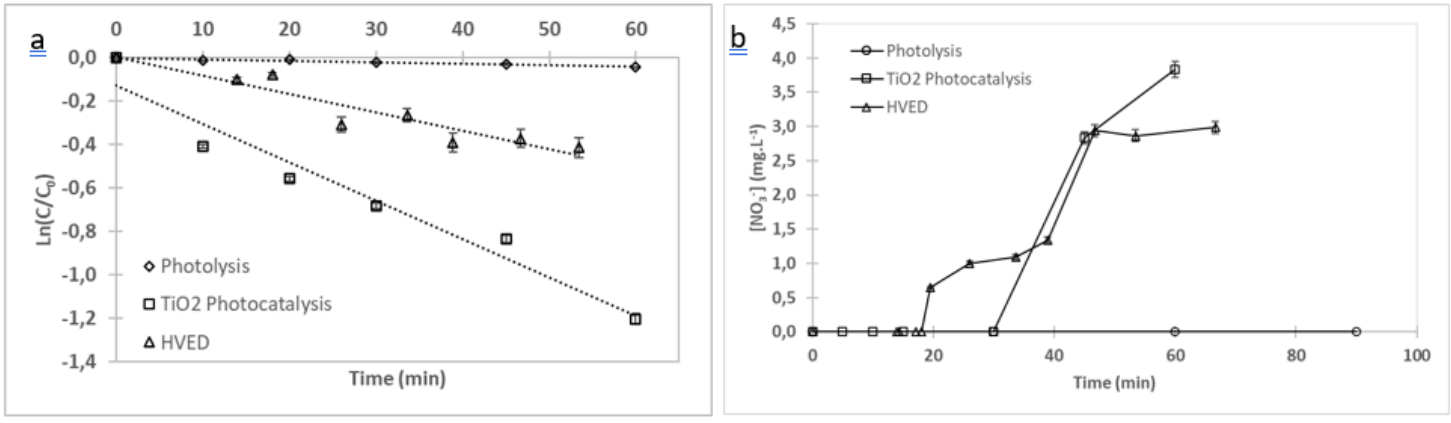

Figure 2

(a) Apparent first-order kinetics for non-purgeable organic carbon and (b) concentration of nitrate ions as a function of reaction time for CIP photolysis, TiO_2 photocatalysis and HVED treatments in synthetic freshwater.

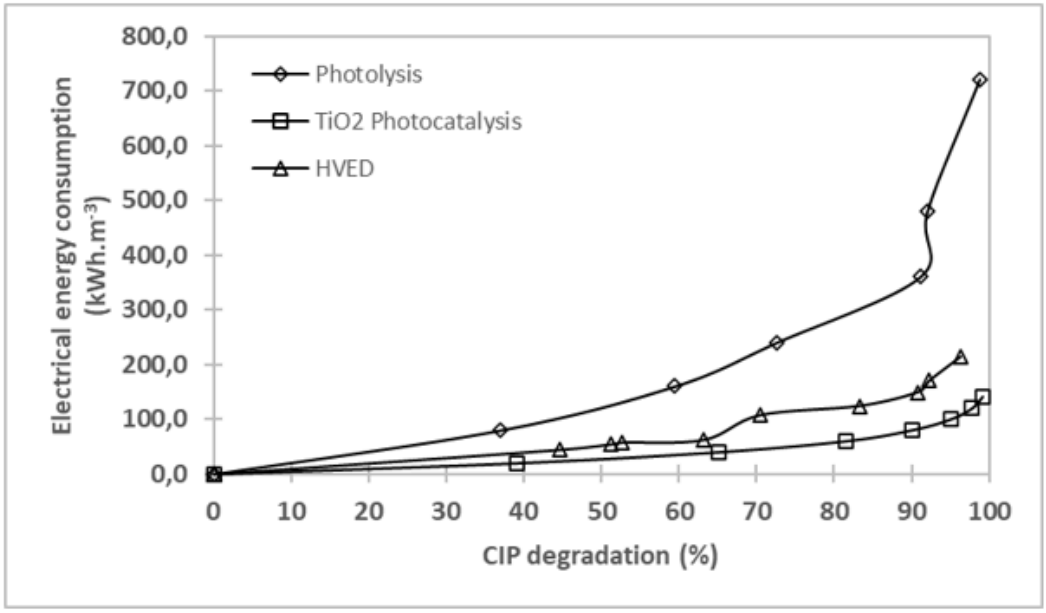

Figure 3

Comparison of the electrical energy consumptions for photolysis, TiO_2 photocatalysis, and HVED treatments as a function of CIP degradation.

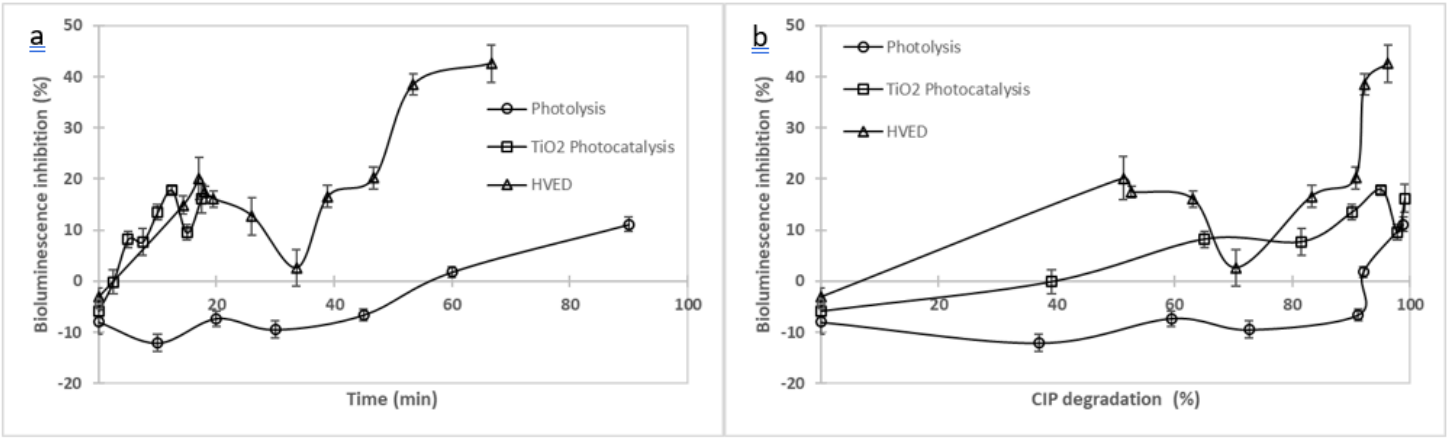

Figure 4

Bioluminescence inhibition of *Vibrio fischeri* (at 30 minutes) as a function of treatment time (a) or CIP degradation (b) for different degradation processes

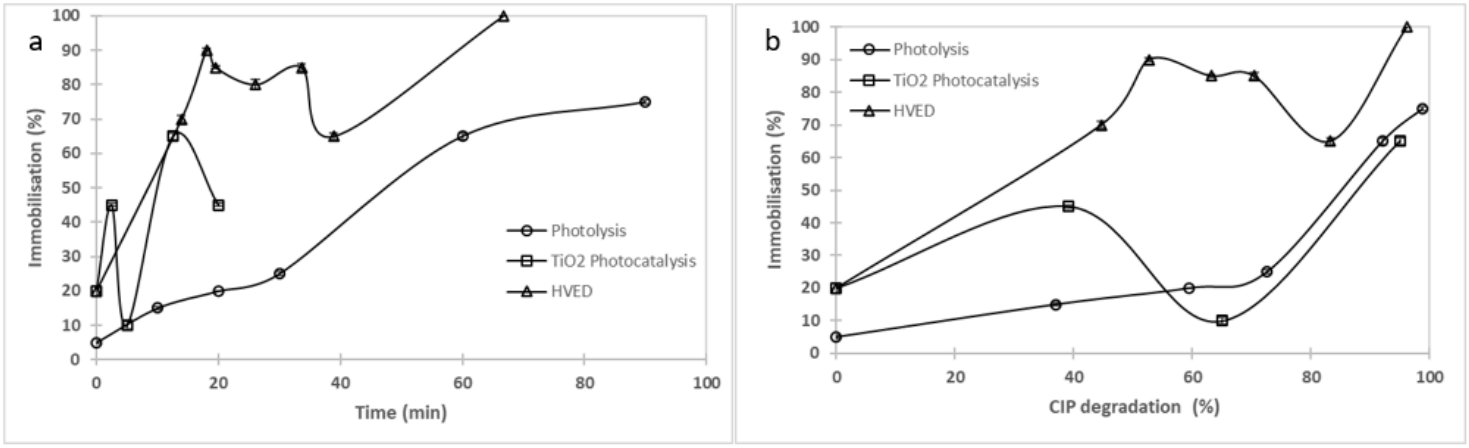

Figure 5

Immobilisation of *Daphnia magna* as a function of treatment time (a) or CIP degradation (b) for different degradation processes

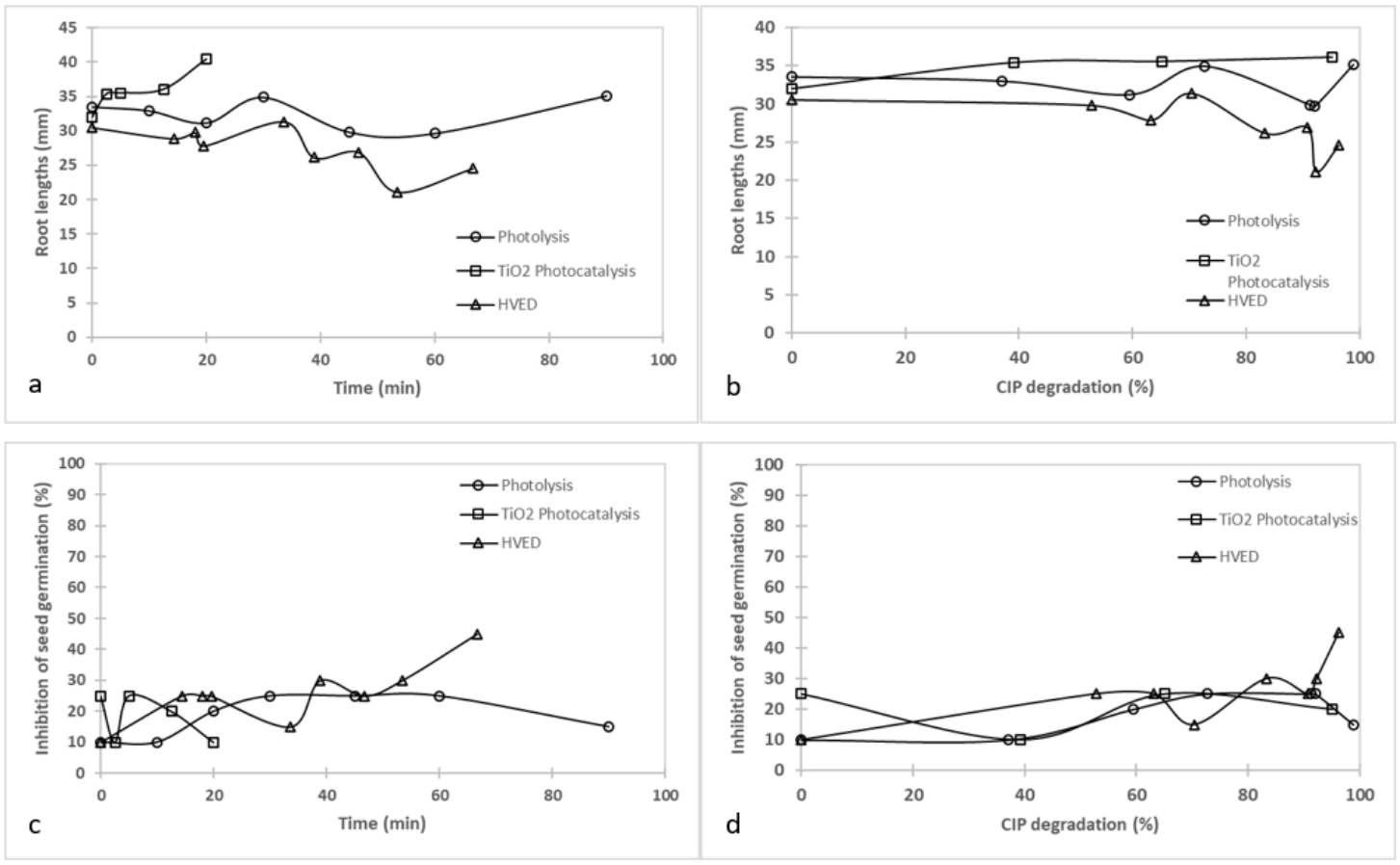

Figure 6

Toxic effects of CIP degradation products on *Trifolium repens*: root growth (a, b) and seed germination inhibition (c, d) as functions of treatment time (a, c) and degradation efficiency (b, d)

Supplementary Files

This is a list of supplementary files associated with this preprint. Click to download.

- ESM1SupplementaryInformation.pdf